

Double sliding window variance detection-based time-of-arrival estimation in ultra-wideband ranging systems

Ibrahim Yassine Nouali¹, Zohra Slimane², Abdelhafid Abdelmalek¹

¹STIC Laboratory, Department of Telecommunications, Faculty of Technology, Tlemcen University, Tlemcen, Chetouane, Algeria

²STIC Laboratory, Electrical Engineering Department, Belhadj Bouchaib University, Ain Temouchent, Algeria

Article Info

Article history:

Received Sep 13, 2021

Revised May 28, 2022

Accepted Jun 25, 2022

Keywords:

Energy detection

Ranging

Sliding window

Time-of-arrival

Ultra-wideband

Variance detection

ABSTRACT

Ultra-wideband (UWB) ranging via time-of-arrival (TOA) estimation method has gained a lot of research interests because it can take full advantage of UWB capabilities. Energy detection (ED) based TOA estimation technique is widely used in the area due to its low cost, low complexity and ease of implementation. However, many factors affect the ranging performance of the ED-based methods, especially, non-line-of-sight (NLOS) condition and the integration interval. In this context, a new TOA estimation method is developed in this paper. Firstly, the received signal is denoised using a five-level wavelet decomposition, next, a double sliding window algorithm is applied to detect the change in the variance information of the received signal, the first path (FP) TOA is then calculated according to the first variance sharp increase. The simulation results using the CM1 and CM2 IEEE 802.15.4a channel models, prove that our proposed approach works effectively compared with the conventional ED-based methods.

This is an open access article under the [CC BY-SA](https://creativecommons.org/licenses/by-sa/4.0/) license.



Corresponding Author:

Ibrahim Yassine Nouali

STIC Laboratory, Department of Telecommunications, Faculty of Technology, Tlemcen University

Tlemcen, Chetouane, Algeria

Email: ibrahimyassine.nouali@univ-tlemcen.dz

1. INTRODUCTION

In recent years, ultra-wideband (UWB) technology has been widely used as a viable solution for indoor position estimation-based applications such as surveillance, navigation, rescue applications, advertising, crowd-sensing and so on [1]–[6]. The main advantage of this technology is its large bandwidth that allows a fine time resolution and a high precision ranging and positioning [7]–[10]. Time-based ranging technique such as time-of-arrival (TOA) estimation is commonly used in UWB ranging systems because it can take full advantage of UWB characteristics [11], [12]. Then, the position can be calculated by geometric and trigonometric techniques using at least three ranging measurements in two-dimensional positioning [13], [14].

The accuracy of the TOA-based ranging technique depends strongly on how precisely the first path (FP) is detected, however, the existence of dense multipath effect and non-line-of-sight (NLOS) condition in indoor environments can make the detection of the FP quite challenging [15]–[17]. A variety of approaches have been proposed to overcome these problems, with some attempting to build mathematical models for range information [18], which is challenging and overly reliant on prior knowledge. Other energy detection (ED) methods, which are based on low cost and low complexity non-coherent receivers such as the maximum energy selection method (MES), and some other threshold crossing (TC) methods [19], [20]. These methods consist of, first, squaring the received signal using a square-law device and then, put it into a finite time integrator to calculate its energy. As shown in Figure 1, the FP TOA is calculated using the maximum energy block in the MES method; however, under NLOS conditions, the FP may not always be the

strongest path, so there is a delay between the maximum energy block and the energy block that contains the FP. As a result, TOA estimation using the maximum energy block leads to significant ranging errors. For TC methods, the FP TOA is calculated based on the first energy block that exceeds a specific threshold, so choosing a suitable threshold is critical for these methods. Furthermore, in NLOS conditions, the FP is sometimes even below the noise level, making detection with traditional thresholds difficult. A variety of modified methods are proposed to calculate the threshold, but many of them are complex [21], [22], requiring prior knowledge or costly computations. In addition, the ED receiver has its own issues that impact the ranging performance such as signal waveform, pulse width, integration interval and noise floor.

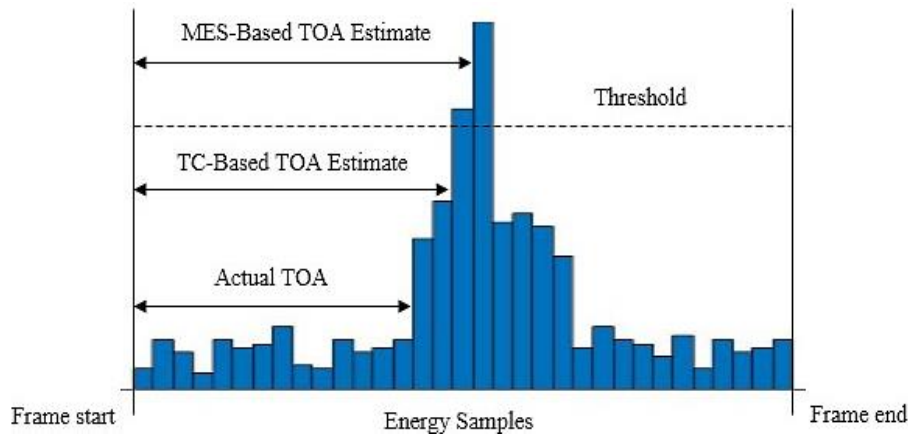


Figure 1. Conventional energy detection-based TOA estimation methods

In this paper, with the aim of improving the limitations of the ED-based methods, we propose a new approach that estimates the FP TOA based on the variance information of the received signal. In this suggested method, a double sliding window variance detection algorithm is deployed and the FP TOA is obtained according to the first variance drastic change. The proposed method is tested using the CM1 and CM2 IEEE 802.15.4a channel models, and the results show a significant accuracy improvement in comparison with the conventional ED-based methods.

The rest of the paper is structured as follows. In section 2, we describe the UWB ranging system model. In section 3, the double sliding window variance detection-based TOA estimation algorithm is presented. Simulations are done in section 4 to compare the performance of the proposed approach with that of the ED-based methods. Section 5 concludes the papers.

2. UWB RANGING SYSTEM MODELS

2.1. Ranging signal

Short time pulse is often used in UWB ranging systems because it offers a very high time resolution with a low energy consumption. Owing to the regulations specified by the Federal Communications Commission (FCC) for UWB transmissions [23]. The Gaussian pulse and its derivatives are widely used as transmitted signals in UWB ranging systems. The second derivative of the Gaussian pulse given in (1), is used as the UWB pulse signal:

$$s(t) = \left(1 - 4\pi \frac{t^2}{\beta^2}\right) e^{\left(\frac{-2\pi t^2}{\beta^2}\right)} \quad (1)$$

where $\beta = 4\pi\sigma^2$ represents the waveform shape factor.

2.2. IEEE 802.15.4a channel model

The IEEE 802.15.4a channel model, as given in [24], is commonly used in the literature for evaluating the performance of UWB ranging systems, it provides different models for different ranges of frequency. Considering our research interest, it may be said that the IEEE 802.15.4a CM1 and CM2 channel models presented in Table 1 may be used to validate the proposed method. Moreover, the IEEE 802.15.4a channel impulse response follows a clustering structure, cluster arrival times are modelled using a Poisson

process and within each cluster, multipath components arrival times are modelled by means of a mixture of Poisson processes. Mathematically, the IEEE 802.15.4a channel impulse response is given by (2):

$$h(t) = \sum_{l=0}^L \sum_{k=0}^K \alpha_{k,l} e^{j\phi_{k,l}} \delta(t - T_l - \tau_{k,l}) \quad (2)$$

where L denotes the number of clusters, K is the number of multipath components in the l th cluster, $\phi_{k,l}$ is the multipath phase distributed uniformly in $[0, 2\pi]$ range and $\alpha_{k,l}$ is the multipath gain. $\tau_{k,l}$ is the delay of the k th multipath component in the l th cluster and T_l is the delay of the l th cluster.

The received signal is given by (3):

$$r(t) = s(t) * h(t) + n(t) \quad (3)$$

where $s(t)$ is the UWB ranging signal, $h(t)$ is the channel impulse response and $n(t)$ is the additive white Gaussian noise (AWGN) with zero mean and power spectral density $N_0/2$. From (1) and (2), the received signal can be expressed as (4).

$$r(t) = \sum_{l=0}^L \sum_{k=0}^K \alpha_{k,l} e^{j\phi_{k,l}} s(t - T_l - \tau_{k,l}) + n(t) \quad (4)$$

Table 1. Description of IEEE 802.15.4a CM1 and CM2 channel models

Channel model number	Environment	Range
CM1	LOS of indoor residential	7 – 20 m
CM2	NLOS of indoor residential	7 – 20 m

2.3. Ranging system performance

For the performance evaluation of our ranging system, the root-mean-squared-error (RMSE) as given in (5) is calculated:

$$RMSE = \sqrt{\sum_{l=1}^S ((\tau_l - \tau_{TOA}) * c)^2 / S} \quad (5)$$

where τ_{TOA} is the true TOA, τ_l is the estimated TOA of each realization, S represents the number of simulations and c is the velocity of the electromagnetic wave. Furthermore, according to the literatures [25], [26] the theoretical accuracy limit of the distance estimation using the TOA method is defined by the Cramer Rao lower bound (CRLB) given in (6):

$$V\{\hat{d}\} \geq \sqrt{\frac{c^2}{8\pi^2 \beta^2 SNR}} \quad (6)$$

where β and \hat{d} are the effective bandwidth of the UWB ranging signal and the estimated distance using the TOA method, respectively. It can be noticed from (6) that the accuracy increases with the bandwidth, which explain the use of UWB signals in ranging systems [27].

2.4. Position calculation

Consider the following scenario: i) a UWB transmitter with unknown location (target node) and three or more UWB receivers with known locations (reference nodes) are placed in a given area and ii) a perfect synchronization between the transmitter and the receivers is guaranteed. The position of the target node is then determined by resolving the (7):

$$\begin{aligned} \sqrt{(x_1 - x_t)^2 + (y_1 - y_t)^2 + (z_1 - z_t)^2} &= \hat{d}_1 \\ \sqrt{(x_2 - x_t)^2 + (y_2 - y_t)^2 + (z_2 - z_t)^2} &= \hat{d}_2 \\ \sqrt{(x_3 - x_t)^2 + (y_3 - y_t)^2 + (z_3 - z_t)^2} &= \hat{d}_3 \\ &\vdots \\ \sqrt{(x_n - x_t)^2 + (y_n - y_t)^2 + (z_n - z_t)^2} &= \hat{d}_n \end{aligned} \quad (7)$$

where (x_n, y_n, z_n) are the known coordinates of the n th reference node, (x_t, y_t, z_t) are the target coordinates and \hat{d}_n is the n th estimated distance between the target node and the n th reference node.

3. DOUBLE SLIDING WINDOW VARIANCE DETECTION-BASED TOA ESTIMATION

The key to UWB TOA-based ranging method is to detect the true first path and estimate its time-of-arrival. The proposed method in this paper aims to capture the change in variance of the received signal to determine the FP TOA. The difference in amplitude between noise samples and noisy signal samples results in a noticeable change in variance at the starting point of signal samples. Thus, the FP TOA can be determined according to the index of the first variance sharp change. In order to achieve this, a double sliding window variance detection algorithm is deployed. The block diagram of the proposed method is given in Figure 2.

The received signal is first denoised using wavelet decomposition. At this stage, a wavelet decomposition is performed on the received signal, and the resulting detailed coefficients, which represent the higher frequency components of the signal at different levels, are thresholded to denoise the signal. There are several algorithms available to estimate the threshold values; however, due to the ease of implementation in the simulation software MATLAB, the minimax algorithm was utilized to find the threshold values. Also, the mother wavelet is vital for improved signal-to-noise separation, and according to [28], standard wavelets that resemble the signal and its properties are chosen as the mother wavelet. The 'sym4' wavelet closely resembles the Gaussian doublet employed in our study; hence, it is selected as the mother wavelet in the denoising process. Following that, the double sliding window variance detection algorithm is employed to identify changes in the variance information of the received denoised signal. It is important to note that the windows size is taken to be less than the guard interval to avoid the overlap between frames of the received signal. The block diagram of the double sliding window algorithm is illustrated in Figure 3, and the detailed steps of the algorithm are outlined below. The received signal can be expressed as $R_{k,n}$, where k is the number of sample and n is the number of frames. Firstly, the received signal is denoised using a five-level wavelet decomposition, the process of denoising is illustrated in Figure 4, where the received signal is presented in Figure 4(a) and the denoised signal is presented in Figure 4(b).



Figure 2. Block diagram of the proposed method



Figure 3. Block diagram of the double sliding window algorithm

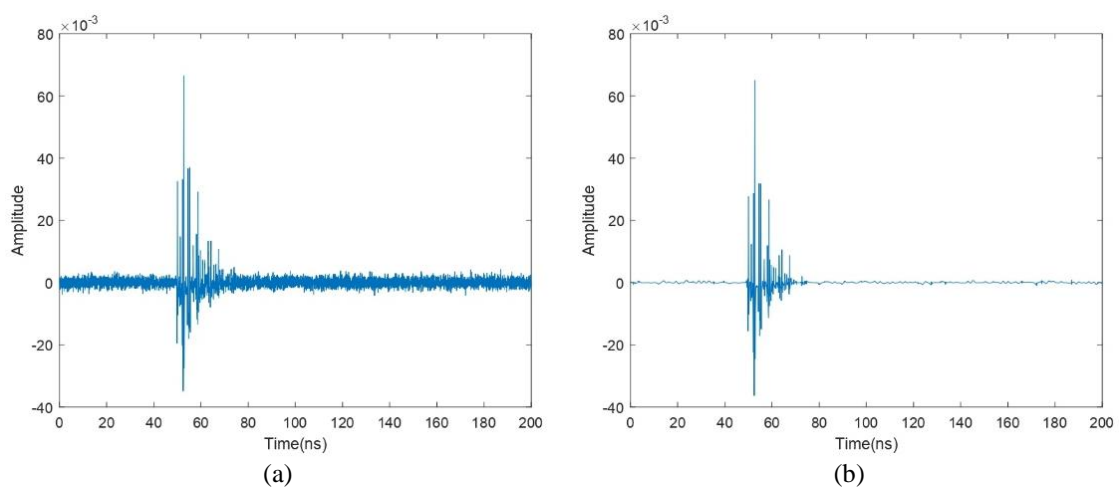


Figure 4. Illustration of the wavelet decomposition based denoising (CM1 channel, SNR = 10 dB);
(a) received signal and (b) denoised signal

The detection of the variance change depends on the variance value in the windows, for the k^{th} sample in the n^{th} frame of the received signal, the variance in the window a is given by (8):

$$a_k = \frac{1}{W} \sum_{k=i}^{W+(k-1)} (R_{k,n} - \mu)^2, i = 1, 2, \dots, K \quad (8)$$

where W is the window size, K is the number of samples and μ is the window mean. To simplify the procedure of detecting the variance change, throughout the entire process of sliding, the variance in the window b is fixed to the variance of a Gaussian random variable x with zero mean and a standard deviation equal to the standard deviation of the received noise, which is estimated from the guard interval. The variance in the window b is given by (9).

$$b_k = \frac{1}{W} \sum_{i=1}^W (x_i)^2, k = 1, 2, \dots, K \quad (9)$$

In order to capture the change in variance of the received signal, a decision function is required, and it is defined as (10).

$$d_k = \frac{a_k}{b_k}, k = 1, 2, \dots, K \quad (10)$$

An illustration of the decision function is given in Figure 5. It can be seen that the decision function peaks at different instants of the received signal. That is because during the process of sliding, the variance in the window a increases and reach its peak at the TOA of each received multipath component. The number of the peaks depends primarily on the size of the window and the delay between the received multipath components, the first peak is a result of the change in variance induced by the FP, and therefore, the FP TOA can be calculated in accordance with the index of the first decision function peak. Mathematically, the index of the first peak is determined using the expression below:

$$k_{toa} = \text{First} \{k | (d_k - d_{k-1}) \geq 0 \text{ and } (d_{k+1} - d_k) \leq 0 \text{ and } d_k > \eta\} \\ k = 2, 3, \dots, K \quad (11)$$

where η is the threshold. For the simplicity of implementation, the threshold is set the root mean square (RMS) of the decision function and it is given by: $\eta = \sqrt{\frac{1}{K} \sum_{k=1}^K d_k^2}$. Finally, the first path time-of-arrival can be calculated using (12):

$$\hat{t}_{toa} = T_s k_{toa} - \tau_{guard} \quad (12)$$

where T_s is the sampling interval and τ_{guard} is the guard interval.

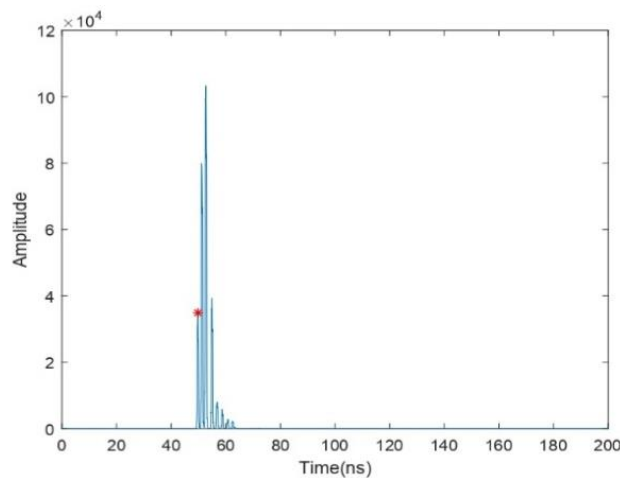


Figure 5. Illustration of the decision function (CM1 channel, SNR = 10 dB)

4. SIMULATION RESULTS AND DISCUSSION

In this section, the performance of the proposed method will be evaluated using the CM1 and CM2 IEEE 802.15.4a channel models. The results presented in Figure 6 were obtained with the following parameters: the UWB ranging signal used is the Gaussian doublet with a pulse duration of 1 ns and a bandwidth of 3.1 GHz, the window size W is 15 samples and S of the RMSE is set to 100 simulations. The number of frames is 200 with a frame duration of 200 ns and SNR ranges from -10 to 20 dB with a step of 5 dB. As far as the conventional energy detection-based methods (MES, TC), according to the simulations done in the literature [19], the width of the energy block for both TC and MES methods is set to 4 ns. MES method selects the center of the maximal energy block as a time-of-arrival and TC method select the center of the first threshold crossing energy block as a time-of-arrival. The threshold selection in the TC method is based on a normalized threshold, given the maximum and the minimum energy values, the normalized threshold is given by (13).

$$\varepsilon_{norm} = \frac{\varepsilon - \min\{E_n\}}{\max\{E_n\} - \min\{E_n\}} \quad (13)$$

In the simulation, the normalized threshold is fixed to 0.6 and the threshold value ε can be calculated from (13). According to the simulation results in Figures 6(a) for CM1 channel and Figure 6(b) for CM2 channel, in all cases, the performance of the proposed method is better than that of any conventional ED-based methods (MES, TC), especially, at high SNR (>-5dB), where the ED-based methods hit an error floor, which is caused by the integration interval. In addition, in NLOS condition, the FP may not be always the strongest path which can cause a higher error floor and significantly reduce the accuracy of the ED-based methods.

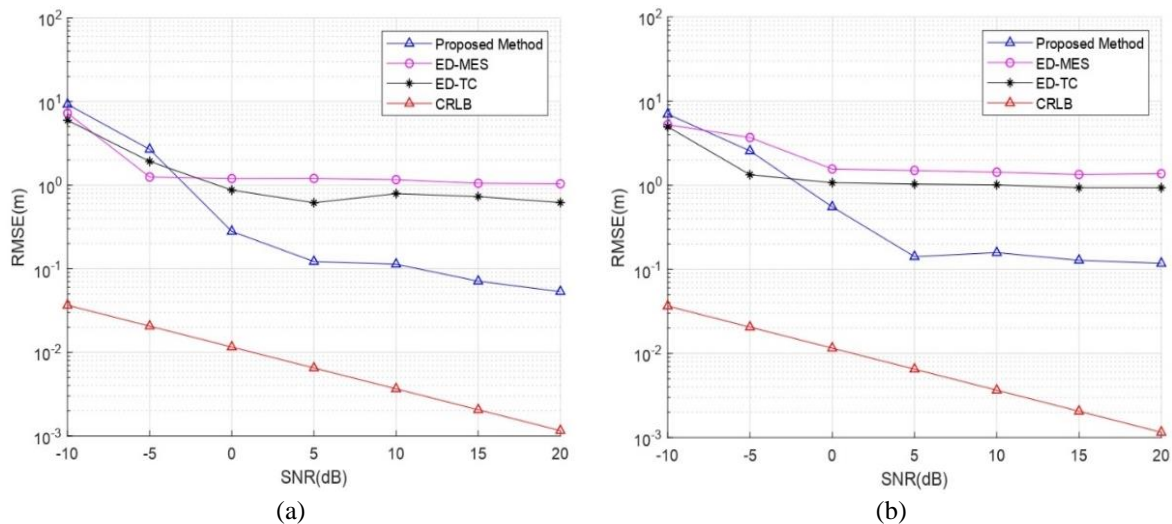


Figure 6. SNR vs RMSE of different approaches in AWGN channel: (a) CM1 and (b) CM2

5. CONCLUSION

Energy detection methods are widely used in UWB ranging systems, nevertheless, the presence of dense multipath effect, NLOS condition, thermal noise and interference can cause large sized errors in the ranging estimation. In this study, we propose a new TOA estimation method that uses a double sliding window algorithm to estimate the FP TOA based on the change in the variance of the received signal. The simulation results with CM1 and CM2 IEEE 802.15.4a channel models proved and confirmed the effectiveness of our proposed approach as compared to the traditional ED-based methods.





REFERENCES

- [1] G. Jekabsons, V. Kairish, and V. Zuravlyov, "An analysis of Wi-Fi based indoor positioning accuracy," *Scientific Journal of Riga Technical University. Computer Sciences*, vol. 44, no. 1, pp. 131–137, Jan. 2011, doi: 10.2478/v10143-011-0031-4.
- [2] K. Al Nuaimi and H. Kamel, "A survey of indoor positioning systems and algorithms," in *2011 International Conference on Innovations in Information Technology*, Apr. 2011, pp. 185–190, doi: 10.1109/INNOVATIONS.2011.5893813.




- [3] K. Witrals *et al.*, "High-accuracy localization for assisted living: 5G systems will turn multipath channels from foe to friend," *IEEE Signal Processing Magazine*, vol. 33, no. 2, pp. 59–70, Mar. 2016, doi: 10.1109/MSP.2015.2504328.
- [4] A. Alarif *et al.*, "Ultra wideband indoor positioning technologies: analysis and recent advances," *Sensors*, vol. 16, no. 5, May 2016, doi: 10.3390/s16050707.
- [5] S. Aditya, A. F. Molisch, and H. M. Behairy, "A survey on the impact of multipath on wideband time-of-arrival based localization," *Proceedings of the IEEE*, vol. 106, no. 7, pp. 1183–1203, Jul. 2018, doi: 10.1109/JPROC.2018.2819638.
- [6] G. Cardone *et al.*, "Fostering participation in smart cities: a geo-social crowdsensing platform," *IEEE Communications Magazine*, vol. 51, no. 6, pp. 112–119, Jun. 2013, doi: 10.1109/MCOM.2013.6525603.
- [7] S. J. Ingram, D. Harmer, and M. Quinlan, "UltraWideBand indoor positioning systems and their use in emergencies," in *PLANS 2004. Position Location and Navigation Symposium (IEEE Cat. No.04CH37556)*, 2004, pp. 706–715, doi: 10.1109/PLANS.2004.1309063.
- [8] I. Guvenc, S. Gezici, and Z. Sahinoglu, "Ultra-wideband range estimation: Theoretical limits and practical algorithms," in *2008 IEEE International Conference on Ultra-Wideband*, Sep. 2008, vol. 3, pp. 93–96, doi: 10.1109/ICUWB.2008.4653424.
- [9] S. Gezici and H. V. Poor, "Position estimation via ultra-wide-band signals," *Proceedings of the IEEE*, vol. 97, no. 2, pp. 386–403, Feb. 2009, doi: 10.1109/JPROC.2008.2008840.
- [10] Z. Sahinoglu, S. Gezici, and I. Guvenc, *Ultra-wideband positioning systems*. Cambridge University Press, 2008.
- [11] Y. Qi, H. Kobayashi, and H. Suda, "Analysis of wireless geolocation in a non-line-of-sight environment," *IEEE Transactions on Wireless Communications*, vol. 5, no. 3, pp. 672–681, Mar. 2006, doi: 10.1109/TWC.2006.1611097.
- [12] S. Gezici *et al.*, "Localization via ultra-wideband radios: a look at positioning aspects for future sensor networks," *IEEE Signal Processing Magazine*, vol. 22, no. 4, pp. 70–84, Jul. 2005, doi: 10.1109/MSP.2005.1458289.
- [13] A. Yassin *et al.*, "Recent advances in indoor localization: A survey on theoretical approaches and applications," *IEEE Communications Surveys & Tutorials*, vol. 19, no. 2, pp. 1327–1346, 2017, doi: 10.1109/COMST.2016.2632427.
- [14] R. F. Brena, J. P. García-Vázquez, C. E. Galván-Tejada, D. Muñoz-Rodríguez, C. Vargas-Rosales, and J. Fangmeyer, "Evolution of indoor positioning technologies: A survey," *Journal of Sensors*, vol. 2017, pp. 1–21, 2017, doi: 10.1155/2017/2630413.
- [15] F. Shang, B. Champagne, and I. Psaromiligkos, "Joint TOA/AOA estimation of IR-UWB signals in the presence of multiuser interference," in *2014 IEEE 15th International Workshop on Signal Processing Advances in Wireless Communications (SPAWC)*, Jun. 2014, pp. 504–508, doi: 10.1109/SPAWC.2014.6941925.
- [16] W. Shi, R. Annavajjala, P. V. Orlik, A. F. Molisch, M. Ochiai, and A. Taira, "Non-coherent ToA estimation for UWB multipath channels using max-eigenvalue detection," in *2012 IEEE International Conference on Communications (ICC)*, Jun. 2012, pp. 4509–4514, doi: 10.1109/ICC.2012.6364618.
- [17] J. R. Foerster, "The effects of multipath interference on the performance of UWB systems in an indoor wireless channel," in *IEEE VTS 53rd Vehicular Technology Conference, Spring 2001. Proceedings (Cat. No.01CH37202)*, 2001, vol. 2, pp. 1176–1180, doi: 10.1109/VETECS.2001.944566.
- [18] S. Bartoletti, W. Dai, A. Conti, and M. Z. Win, "A mathematical model for wideband ranging," *IEEE Journal of Selected Topics in Signal Processing*, vol. 9, no. 2, pp. 216–228, Mar. 2015, doi: 10.1109/JSTSP.2014.2370934.
- [19] Z. Sahinoglu and I. Guvenc, "Threshold-based TOA estimation for impulse radio UWB systems," in *2005 IEEE International Conference on Ultra-Wideband*, 2005, pp. 420–425, doi: 10.1109/ICU.2005.1570024.
- [20] W. Liu and X. Huang, "Analysis of energy detection receiver for TOA estimation in IR UWB ranging and a novel TOA estimation approach," *Journal of Electromagnetic Waves and Applications*, vol. 28, no. 1, pp. 49–63, Jan. 2014, doi: 10.1080/09205071.2013.855149.
- [21] I. Guvenc and Z. Sahinoglu, "Threshold selection for UWB TOA estimation based on kurtosis analysis," *IEEE Communications Letters*, vol. 9, no. 12, pp. 1025–1027, Dec. 2005, doi: 10.1109/LCOMM.2005.1576576.
- [22] X. Wang, B. Yin, Y. Lu, B. Xu, P. Du, and L. Xiao, "Iterative threshold selection for TOA estimation of IR-UWB system," in *2013 IEEE International Conference on Green Computing and Communications and IEEE Internet of Things and IEEE Cyber, Physical and Social Computing*, Aug. 2013, pp. 1763–1766, doi: 10.1109/GreenCom-iThings-CPSCom.2013.324.
- [23] L. S. Committee and others, "Part 15.4: wireless medium access control (MAC) and physical layer (PHY) specifications for low-rate wireless personal area networks (LR-WPANs)," *IEEE Computer Society*, 2003.
- [24] A. F. Molisch *et al.*, "IEEE 802.15. 4a channel model-final report," *IEEE P802*, vol. 15, no. 04, 662, 2004.
- [25] H. Soganci, S. Gezici, and H. Poor, "Accurate positioning in ultra-wideband systems," *IEEE Wireless Communications*, vol. 18, no. 2, pp. 19–27, Apr. 2011, doi: 10.1109/MWC.2011.5751292.
- [26] D. Dardari, A. Conti, U. Ferner, A. Giorgetti, and M. Z. Win, "Ranging with ultrawide bandwidth signals in multipath environments," *Proceedings of the IEEE*, vol. 97, no. 2, pp. 404–426, Feb. 2009, doi: 10.1109/JPROC.2008.2008846.
- [27] J. Xu, C. L. Law, and M. Ma, "Performance of time-difference-of-arrival ultra wideband indoor localisation," *IET Science, Measurement & Technology*, vol. 5, no. 2, pp. 46–53, Mar. 2011, doi: 10.1049/iet-smt.2010.0051.
- [28] M. Srivastava, C. L. Anderson, and J. H. Freed, "A new wavelet denoising method for selecting decomposition levels and noise thresholds," *IEEE Access*, vol. 4, pp. 3862–3877, 2016, doi: 10.1109/ACCESS.2016.2587581.

BIOGRAPHIES OF AUTHORS






Ibrahim Yassine Nouali     received his Master degree in Telecommunication at the University of Tlemcen, (Algeria) in 2018. Currently he is a PhD student at the same University and a member of STIC laboratory. His doctoral research center around ultra-wideband technology and indoor positioning techniques. He can be contacted at email: ibrahimyassine.nouali@univ-tlemcen.dz and nouali.ibrahim.yassine01@gmail.com.



Zohra Slimane    received Magister Diploma (2008), Ph.D. (2012) and HDR (2017), in Telecommunication from Tlemcen University (Algeria). Since 2008, she has been researcher at STIC Laboratory and system engineer at Sonatrach Aval Research Group. In 2014, she joined Belhadj Bouchaïb University Center (Algeria), where she is currently an associate and research Professor, responsible for LMD graduation and doctorate training in the telecommunications sector. Since 2019, she has been involved as project leader dedicated to indoor localization. Her research interests include location and imaging radars, UWB sensors, networking, mobile networks, ubiquitous internet and next-generation networks. She can be contacted at email: zohra.slimane@univ-temouchent.edu.dz and zoh_slimani@yahoo.fr.



Abdelhafid Abdelmalek    received the Laurea degree in Telecommunication Engineering from Institute of Telecommunications Oran (Algeria) in 1991, and Diploma of deepened studies in optoelectronic at Nancy (France) in 1993. From 1994 to 2000, he worked as engineer in charge of design and management of ISDN networks at Algerie Telecoms Company. In 2002, he received Magister Diploma in Signals and systems at Tlemcen University, Algeria. He subsequently joined the faculty of technology and STIC Laboratory as research Professor. He received the Ph.D degree in Electronics in 2013. He has participated in several national research frameworks and projects. His main research activities cover radar, data communications, mobile networks, security, protocols, and high-speed optical networks. He can be contacted at email: abdelmalekabelhafid@gmail.com.